Optics Letters

Chromium/scandium multilayer mirrors for isolated attosecond pulses at 145 eV

Alexander Guggenmos,[1,2,*] Michael Jobst,[2,3] Marcus Ossiander,[2,3] Stefan Radünz,[1,2] Johann Riemensberger,[2,3] Martin Schäffer,[2,3] Ayman Akil,[2] Clemens Jakubeit,[2] Philip Böhm,[4,5] Simon Noever,[4,5] Bert Nickel,[4,5] Reinhard Kienberger,[2,3] and Ulf Kleineberg[1,2]

[1]Fakultät für Physik, Ludwig-Maximilians-Universität München, Am Coulombwall 1, 85748 Garching, Germany
[2]Max-Planck-Institut für Quantenoptik, Hans-Kopfermann-Str. 1, 85748 Garching, Germany
[3]Fakultät für Physik, Technische Universität München, James-Frank-Str. 1, 85748 Garching, Germany
[4]Fakultät für Physik and Center for NanoScience (CeNS), Ludwig-Maximilians-Universität München, Geschwister-Scholl-Platz 1, 80539 München, Germany
[5]Nanosystems Initiative Munich, Schellingstrasse 4, 80799 München, Germany
*Corresponding author: alexander.guggenmos@physik.lmu.de

Received 31 March 2015; revised 21 May 2015; accepted 25 May 2015; posted 26 May 2015 (Doc. ID 237220); published 11 June 2015

Recent advances in the development of attosecond soft x-ray sources toward photon wavelengths below 10 nm are also driving the development of suited broadband multilayer optics for steering and shaping attosecond pulses. We demonstrate that current attosecond experiments in the sub-200-eV range benefit from these improved optics. We present our achievements in utilizing ion-beam-deposited chromium/scandium (Cr/Sc) multilayer mirrors, optimized by tailored material dependent deposition and interface polishing, for the generation of single attosecond pulses from a high-harmonic cut-off spectrum at a central energy of 145 eV. Isolated attosecond pulses have been measured by soft x-ray-pump/NIR-probe electron streaking experiments and characterized using frequency-resolved optical gating for complete reconstruction of attosecond bursts (FROG/CRAB). The results demonstrate that Cr/Sc multilayer mirrors can be used as efficient attosecond optics for reflecting 600-attosecond pulses at a photon energy of 145 eV, which is a prerequisite for present and future attosecond experiments in this energy range.

OCIS codes: (320.0320) Ultrafast optics; (230.4170) Multilayers; (340.7480) X-rays, soft x-rays, extreme ultraviolet (EUV); (230.4040) Mirrors.

http://dx.doi.org/10.1364/OL.40.002846

The development and optimization of highly reflective near-normal incidence multilayer mirror optics for the water window spectral range [1] defined by the K-shell absorption edges of carbon and oxygen (284 and 543 eV, respectively) has been a topic of intensive research over the recent past [2,3]. The driving force is the prospect of high-resolution soft x-ray microscopy [4,5], soft x-ray astronomy [6,7], new optics for soft x-ray free-electron lasers [8], or time-resolved attosecond soft x-ray spectroscopy [9,10]. These multilayer mirrors provide a unique approach for beam steering, spatial and spectral shaping, as well as spectral phase control with reasonably low reflective losses. The most appropriate multilayer material combination in the water window spectral range, above the carbon K-edge and below the scandium L_3-edge, is chromium (Cr) and scandium (Sc) [2,11].

In this Letter, we show that optimizing this material system is not only a key to future attosecond experiments in the water window [12], but also facilitates a promising choice for realizing new attosecond experiments at around 130–160 eV, the energy range where attosecond sources with sufficient photon flux are nowadays already available [13], but multilayer optics are very limited.

The dominating generation process for single isolated attosecond pulses is high harmonic generation (HHG) in gases [14] driven by intense phase-stabilized few-cycle laser pulses [15]. Multilayer mirrors allow for spectral filtering of the broadband high harmonic spectrum in the extreme ultraviolet (XUV)/soft x-ray range with a very high precision upon reflection [16,17]. Central energy and bandwidth of the reflected spectrum can be designed in a flexible manner by the proper choice of layer materials and the multilayer stack design [18]. Figure 1 shows a simulation comparison of certain established multilayer material systems reflecting (attosecond) HHG pulses with a central energy of 145 eV and a full width at half-maximum (FWHM) bandwidth of 3 eV at an angle of normal incidence of 5 degrees; parameters were chosen as a trade-off between spectral and temporal resolution in high-resolution attosecond experiments.

Please note that throughout this manuscript, reflectivity simulations and reflectivity fits have been performed using a Matlab multilayer Fresnel code, which uses tabulated values

of the atomic scattering factors from Henke and Gullikson [19]. The simulations show only a weak suppression of unwanted low-energy out-of-band radiation in the range of ≈120 eV with lanthanum (La)-based multilayer mirrors (La/Mo, La/B_4C); the inevitable and commonly used metal filter for blocking the near-infrared (NIR) laser radiation [typically a 200-nm-thick palladium (Pd) filter] cannot be used to eliminate the out-of-band radiation due to its transmission properties. As a result, chirped plateau harmonics are not sufficiently suppressed by such multilayer reflectors, which is a prerequisite for filtering isolated single-attosecond pulses from the cut-off area of the high harmonic spectrum. This suppression of low-energy out-of-band radiation is essential for attosecond spectroscopy experiments, e.g., delay measurements [20] or direct observation of electron propagation [21]. Well-established molybdenum/silicon (Mo/Si) mirrors, which are widely used in attosecond experiments at photon energies below the silicon L_3-edge at ≈100 eV, suffer from very low reflectivity above 100 eV. Other molybdenum-based multilayer systems like molybdenum/boron carbide (Mo/B_4C), molybdenum/yttrium (Mo/Y), molybdenum/beryllium (Mo/Be), or molybdenum/strontium (Mo/Sr), which on the one hand can provide a higher degree of out-of-band radiation suppression (Mo/B_4C) accompanied with a higher reflectivity (Mo/Y, Mo/Be, Mo/Sr) [22–25] but on the other hand suffer from strong spectral modulations around the main reflectivity Bragg peak by Kiessig fringes and therefore introduce additional group delay dispersion (GDD), which broadens the pulse in the time domain. Furthermore, Mo/Sr is not stable and shows long-term degradation, and beryllium is strongly toxic, thus limiting experimental adoption. A reflection comparison in the time domain of multilayer mirrors composed of Cr/Sc and a high reflective system, here as example Pd/B_4C [26], is shown in the small inset of Fig. 1, which already takes the transmission and the spectral phase of a 200-nm-thick Pd filter into account. Whereas the pulse reflection of the Cr/Sc mirror is close to its Fourier limit and exhibits a Gaussian pulse shape, the Pd/B_4C system shows unwanted temporal pulse broadening due to GDD as well as temporal modulations resulting from the multilayer reflectivity fringes. The Cr/Sc multilayer mirror system, however, combines all the advantages required

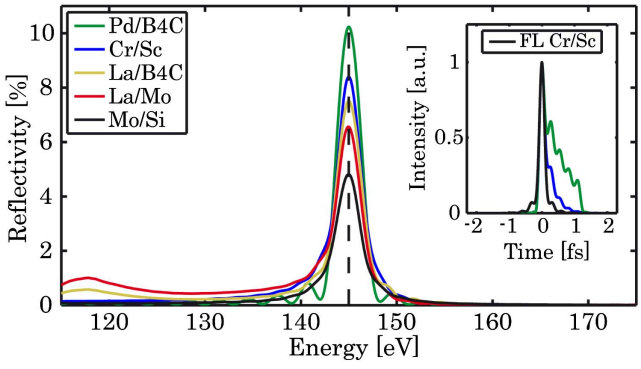

Fig. 1. Simulation comparison of certain multilayer material systems for the reflection of a FWHM bandwidth of 3 eV centered at 145 eV. The small inset shows a comparison of the Cr/Sc and Pd/B_4C system in the time domain including the transmission through a 200-nm-thick palladium (Pd) filter. The black line shows the Fourier limit (FL) of the Cr/Sc mirror reflection.

Table 1. Mirror Parameters

System	d [nm]	γ	σ [nm]	N	Capping
Cr/Sc	4.371	0.4	0.5	65	1.4 nm nat. ox.
La/B_4C	4.402	0.5	0.8	50	—
La/Mo	4.423	0.5	0.4	56	3 nm B_4C
Pd/B_4C	4.402	0.6	0.84	44	—
Mo/Si	4.376	0.5	0.5	60	1.5 nm nat. ox.

for applications with HHG attosecond pulses: sufficient throughput due to the optimized reflectivity [27], suppression of out-of-band radiation components (in case of the lanthanum-based systems a thicker filter can increase the suppression in the 120 eV range but reduces the overall throughput as well), and a nearly (Fourier-limited) Gaussian pulse profile, both in the spectral and temporal domain. The corresponding mirror parameters (period thickness d, ratio γ, interface roughness σ, period number N, and capping) applied in the simulations of Fig. 1, for a bandwidth of 3 eV (FWHM) centered at 145 eV, are depicted in Table 1.

The experimental realization of the Cr/Sc attosecond multilayer mirror was performed by a dual-ion-beam-sputtering technique [12] together with tailored interface polishing [27] for a higher mirror reflectivity.

For a later characterization by attosecond streaking, the mirror was additionally analyzed by two independent measurement techniques, hard x-ray reflectometry and XUV/soft x-ray reflectometry. The hard x-ray reflectometry (XRR) measurement, using a molybdenum K_α source with a wavelength of $\lambda \approx 0.071$ nm, was performed on a flat witness sample, grown on a silicon (100) wafer with a native SiO_2 layer. A comparison of the measured and simulated XRR data of the Cr/Sc attosecond mirror is shown in Fig. 2.

The fitting procedure of the XRR measurement, including the native Cr_2O_3 top layer, reveals only a 0.2% shift of the aimed period thickness and a Nevot–Croce [28] interface roughness of $\sigma = 0.198$ nm since even the 9th Bragg order is well resolved. The 5th Bragg order is not completely suppressed and points to a period thickness ratio of $\gamma = 0.405$. Even though every 10th period (chromium layer) was polished with krypton (Kr) ions [27], the multilayer still shows a pronounced periodicity as indicated by very sharp Bragg peaks. The strong periodicity is the prerequisite for a flat spectral phase upon reflection without additionally introduced GDD.

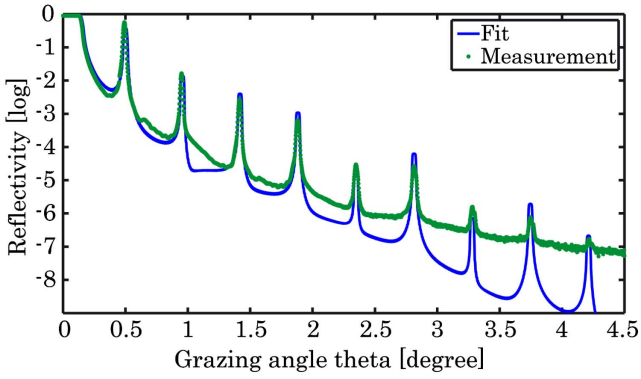

Fig. 2. Hard x-ray reflectometry measurement (green dots) and the fit (solid blue) for the Cr/Sc attosecond mirror.

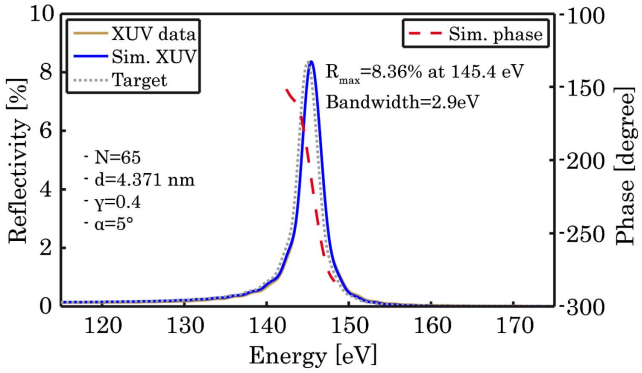

Fig. 3. XUV/soft x-ray reflectometry measurement (solid brown), the corresponding fit (solid blue), and the target design (dotted gray) together with the simulated phase (dashed red).

We have additionally analyzed the Cr/Sc mirror reflectivity at near-normal incidence by XUV/soft x-ray reflectometry, which was performed on a second witness sample. The measured reflectivity profile, together with its simulation and target curve, is shown in Fig. 3.

The Cr/Sc attosecond mirror design exhibits a maximum reflectivity of 8.36% centered at 145.4 eV and reflects over the intended bandwidth of ≈3 eV, as depicted by the solid brown line in Fig. 3. We find a perfect match of the simulation (solid blue) and the measurement, with only a 0.27% shift of the measured peak wavelength from the target wavelength (dotted gray). The XUV/soft x-ray measurement was carried out at the Physikalisch-Technische Bundesanstalt (PTB) beamline at BESSY II in Berlin.

As a final application of this Cr/Sc multilayer mirror to attosecond pulses at 145 eV, an attosecond-electron-streaking experiment was performed to characterize the mirrors temporal attosecond pulse response. High harmonics (HH) have been generated in a neon (Ne) gas jet (200 mbar, <4 fs, 1.5 mJ, $f = 40$ cm), resulting in an HH spectrum with a cut-off energy ranging up to 150 eV, and are then focused by means of a Cr/Sc multilayer-coated double mirror in a second Ne gas jet for photo-ionization.

To characterize the attosecond pulses upon reflection from the Cr/Sc multilayer mirror, we used the well-established XUV/soft x-ray pump/NIR probe-streaking technique [29]. Here, both the attosecond soft x-ray pulse and the NIR laser pulse are focused by a double mirror into neon gas. The soft x-ray pulse photo-ionizes Ne atoms, which frees photoelectrons from the 2p shell, which are then momentum-streaked by the co-propagating temporally synchronized and phase stabilized NIR laser's electric field. The inner part of the double mirror can be moved with respect to the outer part, to introduce a temporal delay between the soft x-ray pulse, which is reflected at the mirror core, and the laser pulse, which is reflected at the outer ring. Changing the delay between the laser and the soft x-ray attosecond pulse yields a typical streaking spectrogram [Fig. 4(a)].

FROG/CRAB [30] analysis allows for a complete reconstruction of both the intensity and the phase of the soft x-ray attosecond pulse, as well as the vector potential of the streaking laser field from a recorded spectrogram [Fig. 4(a)]. Figure 4(b) shows the result of the appropriate FROG/CRAB retrieval as described in [31,32].

Figures 4(c) and 4(d) display the retrieved intensity (solid blue line) and phase (dotted red line) of the soft x-ray pulse, once in the spectral (c) and once in the temporal (d) domain.

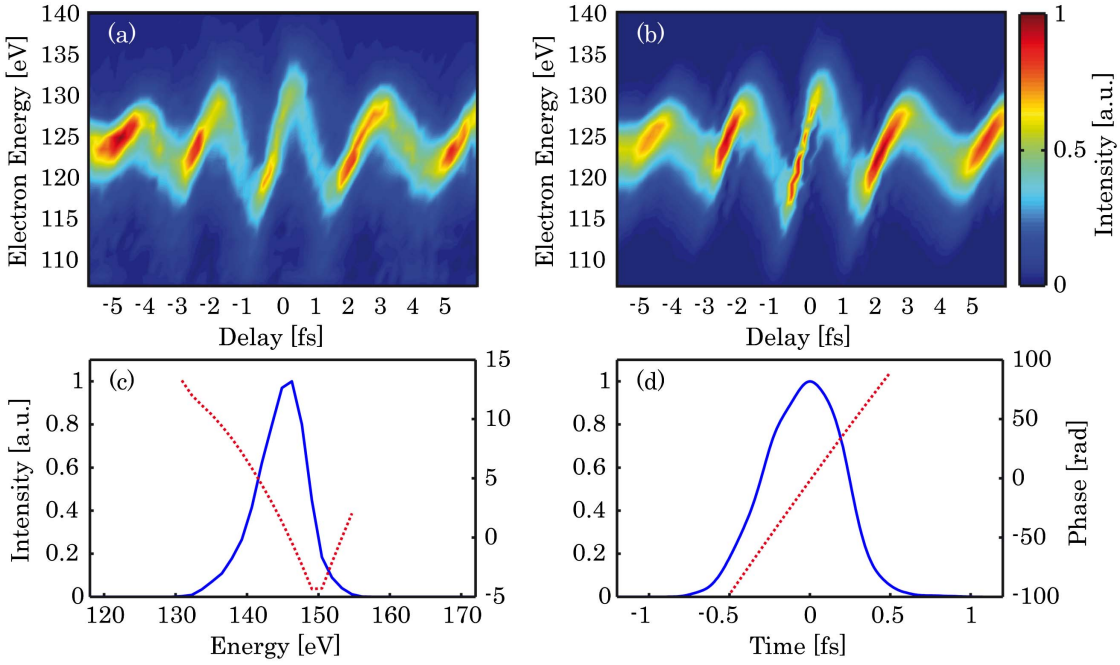

Fig. 4. Cr/Sc multilayer mirror for attosecond pulses. (a)–(d) Results of an attosecond streaking experiment for pulse characterization in neon. (a) Shows the measured electron streaking trace and (b) the retrieved trace performed by FROG/CRAB analyses. (c) The retrieved soft x-ray pulse (solid blue) and the phase (dotted red) in the spectral domain. (d) Soft x-ray pulse and phase in the temporal domain.

Shifted by the binding energy of the Ne-2p electrons (21.6 eV), the soft x-ray pulse shows a central energy of 145.6 eV, which is in good agreement to the target and the previously described results. With the retrieved spectral bandwidth and phase being the most prominent sources of uncertainty, the temporal error can be estimated to be about 20 as. From the retrieved amplitude and phase, we find an attosecond pulse duration of about 580 as in the temporal domain, which is in excellent agreement with the previous estimations (based solely on the mirror reflectivity plus the assumption of a flat mirror phase). A perfect Gaussian Fourier-limited pulse with 2.9 eV bandwidth has a duration of 629 as.

In summary, we have developed and applied an optimized Cr/Sc multilayer mirror for reflecting single isolated attosecond pulses at a photon energy of 145 eV with a pulse duration of 580, which is to the best of our knowledge 27 eV higher than the recent energy limit in tabletop attosecond pump studies [21]. This experimental achievement now paves the way for attosecond experiments above 130 eV, the soft x-ray photon energy range that was not addressed until very recently. The true benefit of this achievement is in its scaling toward the preparation of attosecond pulses at even higher photon energies ranging into the water window spectral range, which will give access to even deeper bound electronic core states and open up new possibilities for attosecond experiments on biomolecules in the foreseen future.

Bundesministerium für Bildung und Forschung (Federal Ministry of Education and Research) (BMBF-05K13WM1); Deutsche Forschungsgemeinschaft (DFG) (EXC158).

We thankfully acknowledge scientific support and valuable discussions by Ferenc Krausz (MPQ, LMU).

REFERENCES

1. C. Spielmann, N. H. Burnett, S. Sartania, R. Koppitsch, M. Schnürer, C. Kan, M. Lenzner, P. Wobrauschek, and F. Krausz, Science **278**, 661 (1997).
2. F. Eriksson, G. A. Johansson, H. M. Hertz, E. M. Gullikson, U. Kreissig, and J. Birch, Opt. Lett. **28**, 2494 (2003).
3. T. Kuhlmann, S. Yulin, T. Feigl, N. Kaiser, T. Gorelik, U. Kaiser, and W. Richter, Appl. Opt. **41**, 2048 (2002).
4. T. Gorniak, R. Heine, A. P. Mancuso, F. Staier, C. Christophis, M. E. Pettitt, A. Sakdinawat, R. Treusch, N. Guerassimova, J. Feldhaus, C. Gutt, G. Grübel, S. Eisebitt, A. Beyer, A. Gölzhäuser, E. Weckert, M. Grunze, I. A. Vartanyants, and A. Rosenhahn, Opt. Express **19**, 11059 (2011).
5. W. Chao, J. Kim, S. Rekawa, P. Fischer, and E. H. Anderson, Opt. Express **17**, 17669 (2009).
6. M. Santos-Lleo, N. Schartel, H. Tananbaum, W. Tucker, and M. C. Weisskopf, Nature **462**, 997 (2009).
7. D. Martínez-Galarce, R. Soufli, D. L. Windt, M. Bruner, E. Gullikson, S. Khatri, E. Spiller, J. C. Robinson, S. Baker, and E. Prast, Opt. Eng. **52**, 095102 (2013).
8. M. Prasciolu, A. F. G. Leontowich, K. R. Beyerlein, and S. Bajt, Appl. Opt. **53**, 2126 (2014).
9. M. Hentschel, R. Kienberger, C. Spielmann, G. A. Reider, N. Milosevic, T. Brabec, P. Corkum, U. Heinzmann, M. Drescher, and F. Krausz, Nature **414**, 509 (2001).
10. M. Schultze, K. Ramasesha, C. D. Pemmaraju, S. A. Sato, D. Whitmore, A. Gandman, J. S. Prell, L. J. Borja, D. Prendergast, K. Yabana, D. M. Neumark, and S. R. Leone, Science **346**, 1348 (2014).
11. F. Schäfers, H.-C. Mertins, F. Schmolla, I. Packe, N. N. Salashchenko, and E. A. Shamov, Appl. Opt. **37**, 719 (1998).
12. A. Guggenmos, R. Rauhut, M. Hofstetter, S. Hertrich, B. Nickel, J. Schmidt, E. M. Gullikson, M. Seibald, W. Schnick, and U. Kleineberg, Opt. Express **21**, 21728 (2013).
13. W. Schweinberger, A. Sommer, E. Bothschafter, J. Li, F. Krausz, R. Kienberger, and M. Schultze, Opt. Lett. **37**, 3573 (2012).
14. T. Popmintchev, M.-C. Chen, D. Popmintchev, P. Arpin, S. Brown, S. Ališauskas, G. Andriukaitis, T. Balciunas, O. D. Mücke, A. Pugzlys, A. Baltuška, B. Shim, S. E. Schrauth, C. Gaeta, L. Plaja, C. Hernández-García, A. Becker, A. Jaron-Becker, M. M. Murnane, and H. C. Kapteyn, Science **336**, 1287 (2012).
15. A. Baltuška, T. Udem, M. Uiberacker, M. Hentschel, E. Goulielmakis, C. Gohle, R. Holzwarth, V. S. Yakovlev, A. Scrinzi, T. W. Hänsch, and F. Krausz, Nature **421**, 611 (2003).
16. M. Hofstetter, M. Schultze, M. Fieß, B. Dennhardt, A. Guggenmos, J. Gagnon, V. Yakovlev, E. Goulielmakis, R. Kienberger, E. M. Gullikson, F. Krausz, and U. Kleineberg, Opt. Express **19**, 1767 (2011).
17. C. Bourassin-Bouchet, S. de Rossi, J. Wang, E. Meltchakov, A. Giglia, N. Mahne, S. Nannarone, and F. Delmotte, New J. Phys. **14**, 023040 (2012).
18. M. Hofstetter, A. Aquila, M. Schultze, A. Guggenmos, S. Yang, E. Gullikson, M. Huth, B. Nickel, J. Gagnon, V. S. Yakovlev, E. Goulielmakis, F. Krausz, and U. Kleineberg, New J. Phys. **13**, 063038 (2011).
19. B. L. Henke, E. M. Gullikson, and J. C. Davis, At. Data Nucl. Data Tables **54**, 181 (1993).
20. M. Schultze, M. Fieß, N. Karpowicz, J. Gagnon, M. Korbman, M. Hofstetter, S. Neppl, A. L. Cavalieri, Y. Komninos, T. Mercouris, C. A. Nicolaides, R. Pazourek, S. Nagele, J. Feist, J. Burgdörfer, A. M. Azzeer, R. Ernstorfer, R. Kienberger, U. Kleineberg, E. Goulielmakis, F. Krausz, and V. S. Yakovlev, Science **328**, 1658 (2010).
21. S. Neppl, R. Ernstorfer, A. L. Cavalieri, C. Lemell, G. Wachter, E. Magerl, E. M. Bothschafter, M. Jobst, M. Hofstetter, U. Kleineberg, J. V. Barth, D. Menzel, J. Burgdörfer, P. Feulner, F. Krausz, and R. Kienberger, Nature **517**, 342 (2015).
22. C. Montcalm, B. T. Sullivan, S. Duguay, M. Ranger, W. Steffens, H. Pépin, and M. Chaker, Opt. Lett. **20**, 1450 (1995).
23. R. Soufli, E. Spiller, D. L. Windt, J. C. Robinson, E. M. Gullikson, L. R. Marcos, M. Fernández-Perea, S. L. Baker, A. L. Aquila, F. J. Dollar, J. A. Méndez, J. I. Larruquert, L. Golub, and P. Boerner, Proc. SPIE **8443**, 84433C (2012).
24. S. Bajt, J. Vac. Sci. Technol. A **18**, 557 (2000).
25. B. Sae-Lao and C. Montcalm, Opt. Lett. **26**, 468 (2001).
26. C. Montcalm, P. A. Kearney, J. M. Slaughter, B. T. Sullivan, M. Chaker, H. Pépin, and C. M. Falco, Appl. Opt. **35**, 5134 (1996).
27. A. Guggenmos, S. Radünz, R. Rauhut, M. Hofstetter, S. Venkatesan, A. Wochnik, E. M. Gullikson, S. Fischer, B. Nickel, C. Scheu, and U. Kleineberg, Opt. Express **22**, 26526 (2014).
28. L. Névot and P. Croce, Rev. Phys. Appl. **15**, 761 (1980).
29. R. Kienberger, E. Goulielmakis, M. Uiberacker, A. Baltuska, V. Yakovlev, F. Bammer, A. Scrinzi, T. Westerwalbesloh, U. Kleineberg, U. Heinzmann, M. Drescher, and F. Krausz, Nature **427**, 817 (2004).
30. R. Trebino, K. W. DeLong, D. N. Fittinghoff, J. N. Sweetser, M. A. Krumbügel, B. A. Richman, and D. J. Kane, Rev. Sci. Instrum. **68**, 3277 (1997).
31. J. Gagnon and V. S. Yakovlev, Opt. Express **17**, 17678 (2009).
32. J. Gagnon, E. Goulielmakis, and V. S. Yakovlev, Appl. Phys. B **92**, 25 (2008).